United States Department of Agriculture | **Natural Resources Conservation Service** | **11 Campus Boulevard, Suite 200 Newtown Square, PA 19073**

Subject: SOI – Geophysical Field Assistance **Date:** 6 April 2005

To: Dr. Henry Lin
Assistant Professor of Hydropedology/Soil Hydrology
Crop & Soil Sciences Department
415 Agricultural Sciences and Industries Building
Pennsylvania State University
University Park, PA 16802

Edgar White
State Soil Scientist
USDA-NRCS
One Credit Union Place, Suite 340
Harrisburg, PA 17110-2993

Purpose:
Electromagnetic induction (EMI) and ground-penetrating radar (GPR) were used to assist the Pennsylvania State University's Hydropedology Team assess spatial variations in soils and soil properties within a small, steeply sloping, forested watershed in central Pennsylvania.

Participants:
Jim Doolittle, Research Soil Scientist, USDA-NRCS-NSSC, Newtown Square, PA
Yuri Plowden, Soil Scientist, USDA-NRCS, University Park, PA

Activities:
All field activities were completed on 8 and 9 March 2005.

Summary:

1. This study represents the first know use of electromagnetic induction and ground-penetrating radar to characterize the hydropedology of a forested watershed. These tools were found to be complimentary and their integrated use advantageous to hydropedologic studies.

2. Protocol for conducting geophysical surveys in steeply sloping, forested terrains requires refinement. Electromagnetic induction can be used as a rapid reconnaissance tool to survey small watersheds. However, intricate soil patterns and different landscape components require intensive sampling. Ground-penetrating radar can be used to provide high resolution data of select areas. However, multiple, discontinuous reflectors complicate interpretations and low amplitude reflectors foster ambiguities. Terrains are often difficult to traverse with geophysical tools and the use of GPS to position data is restricted in steeply sloping, forested areas.

3. Within the Shale Hills Watershed, distinct soil/landscape components have been recognized. The models used to map soils within the watershed were confirmed by geophysical methods. Electromagnetic induction was used to map the principal soil/landscape components within the watershed. Ground-penetrating radar provided comprehensive data on soil depth and characterized alluvial deposits within recesses (swales). Strata within colluvial deposits that were identified with GPR were not described by soil scientists in excavated pits. In recesses and in areas of Rushtown (and probably Berks) soils, layers of colluvium occur and influence the movement of soil water. These layers need to be more adequately described (see pedon descriptions in

compendium to this report).

4. I feel that much has been learned in this experience. The lessons learned in this study need to be applied and examined by others.

It was my pleasure to participate in this study and to work with Yuri and the faculty of Pennsylvania State University.

With kind regards,

James A. Doolittle
Research Soil Scientist
National Soil Survey Center

cc:
B. Ahrens, Director, USDA-NRCS, National Soil Survey Center, Federal Building, Room 152, 100 Centennial Mall North, Lincoln, NE 68508-3866
S. Carpenter, MLRA Office Leader, USDA-NRCS, 75 High Street, Room 301, Morgantown, WV 26505
M. Golden, Director of Soils Survey Division, USDA-NRCS, Room 4250 South Building, 14th & Independence Ave. SW, Washington, DC 20250
D. Hammer, National Leader, Soil Investigation Staff, USDA-NRCS, National Soil Survey Center, Federal Building, Room 152, 100 Centennial Mall North, Lincoln, NE 68508-3866
W. Tuttle, Soil Scientist (Geophysical), USDA-NRCS, National Soil Survey Center, P.O. Box 60, 207 West Main Street, Rm. G-08, Federal Building
Wilkesboro, NC 28697

Introduction:
Variable and anisotropic soil properties complicate soil mapping, interpretation, and modeling. Traditional methods of soil investigation provide accurate and detailed information about soil properties at specific points of observation. However, these methods are slow, labor-intensive, and expensive. As a consequence, traditional methods of soil investigation can only provide a limited number of observations, sparse coverage of soil polygons, and frequently do not fully characterize the variability of soils and soil properties. New tools are needed to characterize the variability of soils and soil properties. Because of their speed and ease of use, electromagnetic induction (EMI) and ground-penetration radar (GPR) provide a greater number of measurements and more comprehensive coverage of soil polygons than traditional tools or methods. The use of EMI and GPR can greatly improve the effectiveness of hydropedologic investigations by reducing the number and improving the placement of soil cores, and providing additional information on soils and soil properties.

Electromagnetic induction operates by inducing circular eddy current loops into the soil and measuring the magnitudes of the electromagnetic energy in these loops. Under certain conditions (known as operating at low induction numbers), the magnitude of energy in these current loops is proportional to the apparent conductivity (EC_a) of soil materials near the current loops. Apparent conductivity is a weighted, average conductivity measurement for a column of earthen materials to a specific depth (Greenhouse and Slaine, 1983). Variations in EC_a are produced by changes in the electrical conductivity of earthen materials. Interpretations of EMI data are based on the identification of spatial patterns within data sets. Though seldom diagnostic in themselves, lateral and vertical variations in EC_a have been used to infer changes in soils and soil properties (Kravchenko et al., 2002; Doolittle et al., 1996 and 1994; Sudduth et al., 1995; Jaynes et al., 1993). In many areas, EC_a patterns correspond well with soil patterns shown on soil maps. Because of the greater number of measurements, maps prepared from EMI data can provide higher levels of resolution than soil maps prepared with traditional tools or survey methods (Jaynes, 1995).

Ground-penetrating radar is an impulse radar system designed for shallow, subsurface investigations. Compared with other geophysical techniques, GPR provides very high resolution of subsurface features. Ground-penetrating radar operates by transmitting short pulses of electromagnetic energy into the ground from an antenna. When a pulse of radiated electromagnetic energy contacts an interface separating layers of differing dielectric properties, a portion of the energy is reflected back to a receiving antenna. The time delay between the transmitted pulse and the reflected energy is proportional to the depth to a subsurface interface, which generated the reflection. Ground-penetrating radar has been used to estimate the depth to soil horizons (Daniels, 2004; and Doolittle, 1987), parent rock (Collins et al., 1989; Davis and Annan, 1989; Olson and Doolittle, 1985), and water tables in coarse-textured materials (Doolittle et al., 2000; Iivari and Doolittle, 1994; Bohling et al., 1989).

Electromagnetic induction and ground-penetrating radar are complimentary geophysical tools. Both EMI and GPR respond to the electrical conductivity of soils. The electrical conductivity of soils is influenced by the amount and type of salts in solution, amount and type of clays, porosity, and degree of water saturation. Though both tools are widely used, EMI is generally more suited to investigations over conductive soils that have contrasting electrical properties. The greater the contrasts in electrical conductivity between soils or soil horizons, the more apparent and easily interpreted are the spatial patterns appearing on plots of EMI data. Ground-penetrating radar is most effective in resistive soils. Soils having high electrical conductivity are considered unsuitable to GPR. These soils rapidly dissipate the radar's energy, restrict penetration depths, and create low signal to noise ratios, which greatly impair the quality and interpretability of reflections on radar records. The penetration depth and effectiveness of GPR decreases with increasing soluble salt, clay, and water contents.

Each tool has strengths and weaknesses. Electromagnetic induction can be used as a rapid reconnaissance tool to cover large areas. The processing and interpretation of EMI data are relatively quick and uncomplicated. The collection, processing, and interpretation of GPR data are more time-consuming and complicated. As a consequence, GPR surveys of large areas are considered unreasonable. However, when smaller, more manageable areas have been identified by other techniques, the use of GPR is reasonable and appropriate.

When possible, the use of more than one geophysical method provides complementary and expanded information, which helps to improve and confirm interpretations. A critical point in any integrated geophysical survey is the use of the most suitable and complimentary tools. Methods should complement one another in respect to their ease of use, site coverage,

sensitivity to soil and hydropedologic properties, and resolution of subsurface features. Ground penetrating radar and electromagnetic induction are two such tools. Ground-penetrating radar and electromagnetic induction have been used in tandem to provide subsurface soil information that complements data derived with traditional soil survey methods (Inman et al., 2002; Stroh et al., 2001). Frequently, EMI has been used as a reconnaissance tool to quickly cover relatively large areas. Once the underlying factors for the spatial patterns appearing on plots of EC_a data are identified, GPR surveys can be conducted over selected, smaller areas to provide high-resolution subsurface data. This paper documents the integrated use of two geophysical methods, EMI and GPR, to provide ancillary data on spatial variations in soils and soil properties within a small, steeply sloping, forested watershed in central Pennsylvania. The use of these tools to characterize soil and hydrologic conditions in a forested watershed underlain by resistive materials has not been previously established.

Study Area:

The Shale Hills Watershed is located in northern Huntingdon County. The watershed is in the Ridge and Valley Province of central Pennsylvania. In 1961, the USDA-Forest Service established the Shale Hills Watershed Unit as a long-term forest research site. This forested watershed is relatively small (7.8 ha) and well defined. An oak-hickory cover type dominates most of the watershed. However, an oak-hemlock community exists along the lower reaches of the stream that drains the watershed. The relative topography of the watershed is shown in Figure 1. Within the watershed, elevations range from about 260 to 312 m. Slopes are gently sloping to steep. In Figure 1, the segmented line approximates the location of a small stream that drains the watershed. Within the watershed, a continuous flow of water is maintained throughout the year only along the lower reach of this stream. The watershed is underlain by the Silurian Rose Hill shale formation. The strata are thinly bedded and steeply inclined.

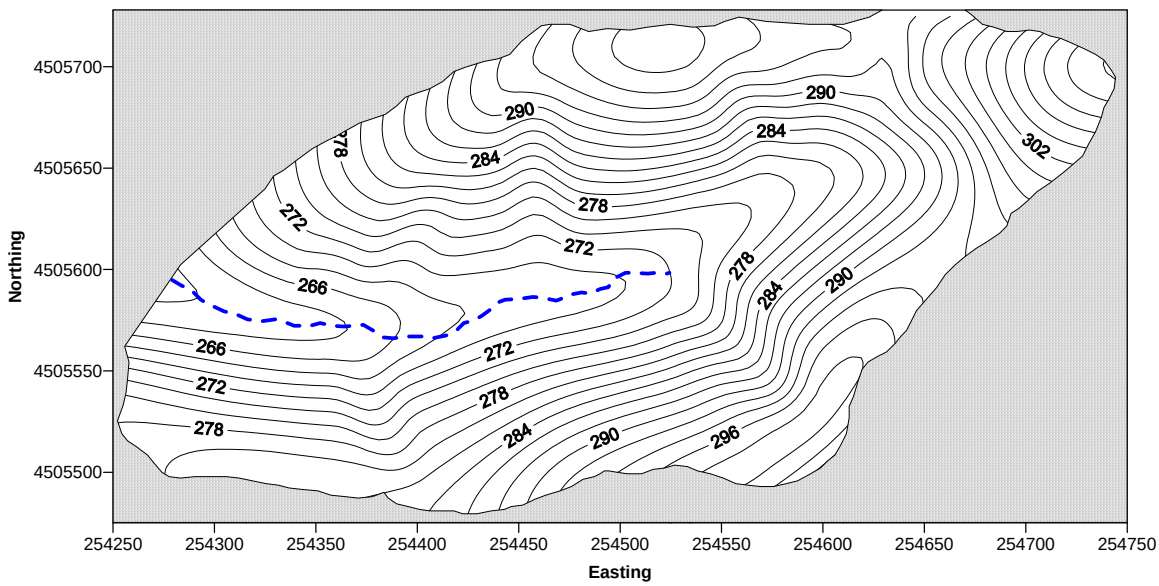

Figure 1. Relative topography of the Shale Hills Watershed.

A majority of the watershed was mapped as Berks-Weikert soils, steep, and Ernest channery silt loam, 3 to 8 percent slopes (Merkel, 1978). The watershed also includes small areas of Berks-Weikert shaly silt loam, 15 to 25 percent slopes, and Berks shaly silt loam, 8 to 15 percent slopes (Merkel, 1978). These soils formed in materials weathered from shale. Table 1 lists the taxonomic classification of the soils mapped within the watershed. The well drained, shallow (25 to 50 cm) Weikert and moderately deep (50-100 cm) Berks soils were mapped on higher-lying, more sloping areas of the watershed. The very deep (> 150cm), moderately well drained Ernest soil was mapped on lower-lying, gently sloping areas along the drainageway. Ernest soil has a fragipan within depths of about 50 to 90 cm.

Table 1. Taxonomic classification of soils

Series	Taxonomic Classification
Berks	loamy-skeletal, mixed, active, mesic Typic Dystrudepts
Blairton	fine-loamy, mixed, active, mesic Aquic Hapludults
Earnest	fine-loamy, mixed, superactive, mesic Aquic Fragiudults
Rushtown	loamy-skeletal over fragmental, mixed, active, mesic Typic Dystrudepts
Weikert	loamy-skeletal, mixed, active, mesic Lithic Dystrudepts

In 2003, a high-intensity soil survey was completed of the watershed. Compared with the earlier order-two soil survey, the high-intensity soil survey recognized of a greater number of soils and soil polygons. The larger scale of the high-intensity soil survey enabled the identification of more intricate soil/landscape components within the watershed. On the high-intensity soil map (Figure 2), Weikert soil dominates the watershed. Earnest and Blairton soils are restricted to the main drainageway. The moderately deep, somewhat poorly drained and moderately well drained Blairton soil forms a minor soil polygon near the drainage head. Berks and Rushtown soils have been mapped in the prominent lower-order drainageways, indentations, or recesses (referred to as swales) of the watershed. The very deep, excessively drained Rushtown soil occurs on the less sloping, concave floors and the Berks soil occurs on the more sloping, plane and convex side slopes of these features. The Berks soil forms in residuum and Rushtown soil forms in colluvium weathered from shale and siltstone. These soils contain large amounts of rock fragments and have varying depths to thinly bedded and highly fractured shale.

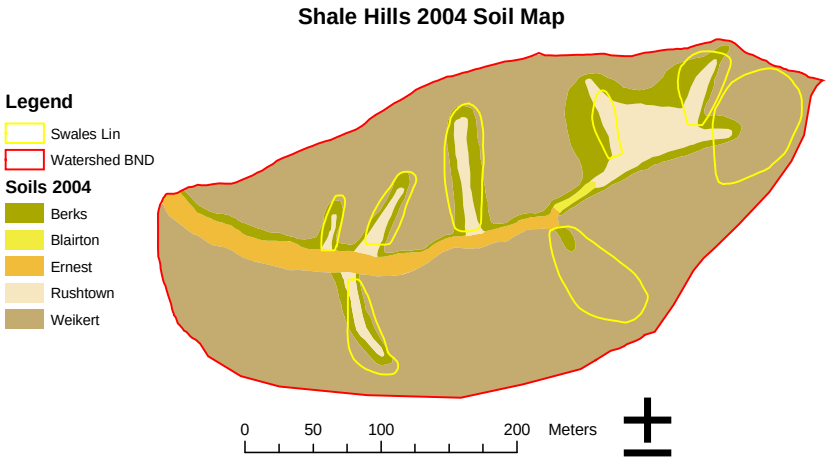

Figure 2. High-intensity soil survey of the Shale Hills Watershed.

Materials and Methods:

An EM38 meter, manufactured by Geonics limited (Mississauga, Ontario) was used in this study.[1] This meter weighs about 1.4 kg (3.1 lbs) and needs only one person to operate. No ground contact is required with this instrument. The EM38 meter has a 1-m intercoil spacing and operates at a frequency of 14,600 Hz. When placed on the soil surface, it has effective penetration depths of about 0.75 and 1.5 m in the horizontal and vertical dipole orientations, respectively (Geonics Limited, 1998). The meter measures the EC_a of the underlying earthen materials. Values of EC_a are expressed in milliSiemens per meter (mS/m).

The Geonics DAS70 Data Acquisition System was used with the EM38 meter to record and store both EC_a and position data.[1] The acquisition system consists of the EM38 meter, an Allegro field computer, and a Garmin Global Positioning System (GPS) Map 76 receiver (with a CSI Radio Beacon receiver, antenna, and accessories that are fitted into a

[1] Manufacturer's names are provided for specific information; use does not constitute endorsement.

backpack). When attached to the acquisition system, the EM38 meter is keypad operated and measurements can be automatically triggered.

To help summarize the results of EMI surveys, the SURFER for Windows, version 8.0, developed by Golden Software, Inc., was used to construct two- and three-dimensional simulations.[1] Grids of EC_a data were created using kriging methods with an octant search.

The radar unit is the TerraSIRch Subsurface Interface Radar (SIR) System-3000 (here after referred to as the SIR System-3000), manufactured by Geophysical Survey Systems, Inc. (North Salem, New Hampshire).[1] The SIR System-3000 consists of a digital control unit (DC-3000) with keypad, SVGA video screen, and connector panel. The SIR System-3000 weighs about 4.1 kg (9 lbs) and is backpack portable. With an antenna, this system requires two people to operate. The 200 and 400 MHz antennas were used in this study.

The RADAN for Windows (version 5.0) software program developed by Geophysical Survey Systems, Inc, was used to process the radar records.[1] Processing included setting the initial pulse to time zero, color table and transformation selection, marker editing, distance normalization, range gain adjustments, migration, and surface normalization. All radar records were migrated to remove hyperbola diffractions and to correct the geometry of inclined soil horizons and stratigraphic or lithologic layers. Surface normalization corrects the radar record for changes in elevation and, in this study, greatly improved interpretations and the association of subsurface reflectors with soils and landscape components.

Survey Procedures:
The EM38 meter was operated in the vertical dipole orientation and continuous mode with measurements recorded at a 1-sec interval. The meter was generally orientated with its long axis parallel to the direction of traverse. When possible, the meter was held about 5 cm (2 inches) above the ground surface. However, steep slopes, tree limbs, and fallen forest debris made walking difficult and caused the meter to be occasionally jostled and varied slightly in surveying height. Where possible, traverses were conducted parallel with the contours. Demanding physical exertion and harsh terrains necessitated frequent pauses of the survey. Horizon obstructions, satellite shading, and multipath reception reduced the accuracy and reliability of GPS positioning on lower slopes within the watershed especially beneath the evergreen canopy along the lower reach of the stream. The locations of the EMI traverses and observation points are shown in Figure 3.

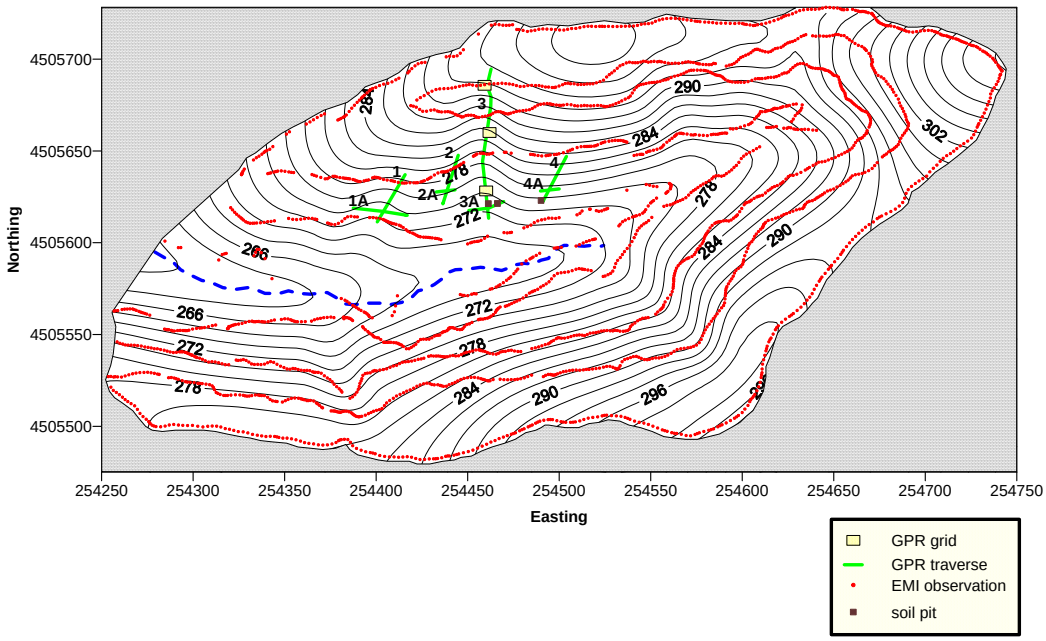

Figure 3. The locations of EMI observations and GPR traverse lines and grids.

Ground-penetrating radar traverses were completed along selected lines established across different landscape

components and soil polygons on the south-facing slopes of the watershed. Four traverse lines were established on two prominent indentations or linear recesses that contained polygons of Rushtown and Berks soils. In Figure 3, these GPR traverse lines are identified as 1, 1A, 3, and 3A. Two of these traverse lines were parallel and two were orthogonal to the long axes of the recesses. Four traverse lines were also located on two linear side slopes that were mapped as Weikert soil. In Figure 3, these GPR traverse lines are identified as 2, 2A, 4, and 4A. Two of these traverse lines were parallel and two were orthogonal to the long axes of the slopes. Along each line, reference flags were inserted in the ground at intervals of 3 m. Pulling the 200 MHz antenna along each line completed a GPR transect. Along each line, as the antenna was towed passed a reference point, a vertical mark was impressed on the radar record. These marks referenced known positions.

To more fully evaluate the three dimensional variability of soils within recesses, three grids were established on different slope components along traverse line 3. Each grid was 5- x 5-m. The grid interval was 50 cm along the Y (orthogonal to slope) axis and 100 cm along the X (parallel with slope) axis, respectively. Pulling the 400 MHz antenna along eleven equally spaced (50 cm), parallel lines completed the GPR survey of each grid. Each traverse line was 5 m long with reference points spaced at 100 cm intervals. As the antenna was towed passed each reference point, a vertical mark was impressed on the radar record. Walking, in a back and forth manner, along the lines completed a GPR survey.

Based on the delineated soil polygons (Figure 2) and inferences drawn from the geophysical surveys, three pits were excavated to better characterize the soils along radar traverse lines 3A and 4 (Figure3). Along line 3A, pits were excavated in areas of Berks (Pedon # 04PA061003) and Rushtown (Pedon # 04PA061002) soils in a recess. The pit excavated at the lower terminus of line 4 was in an area of Weikert (Pedon # 04PA061004) soil on linear side slopes. The compendium to this report contains the descriptions of these soils.

Calibration of GPR:

Ground-penetrating radar is a time scaled system. This system measures the time that it takes electromagnetic energy to travel from an antenna to an interface (e.g., bedrock, soil horizon, stratigraphic layer) and back. To convert the travel time into a depth scale, either the velocity of pulse propagation or the depth to a reflector must be known. The relationships among depth (D), two-way pulse travel time (T), and velocity of propagation (V) are described in the following equation (Daniels, 2004):

$$V = 2D/T \qquad [1]$$

The velocity of propagation is principally affected by the relative permittivity (E_r) of the profiled material(s) according to the equation:

$$E_r = (C/V)^2 \qquad [2]$$

where “C” is the velocity of propagation in a vacuum (0.2998 m/nanosecond). Velocity is expressed in meters per nanosecond (ns). The velocity of propagation is slowed by increases in soil moisture and relative permittivity.

The velocity of propagation is temporally and spatially variable. Soils on side slopes were relatively moist and dry at the time of the GPR traverse and grid surveys, respectively. For each survey, based on the depth to a known, buried reflector and hyperbola-matching processing techniques (the shape of a hyperbole is dependent on the velocity), an averaged velocity of propagation was determined. At the time of the GPR traverse surveys, the velocity of propagation averaged about 0.07 m/ns (E_r of 16.8) on side slopes. At the time of the GPR grid surveys, the velocity of propagation averaged about 0.11 m/ns (E_r of 7.3) on side slopes.

Results:

<u>EMI Survey:</u>

Figure 4 is a two-dimensional plot of EC_a that has been overlain on a three-dimensional surface net diagram of the watershed. In this plot, the EC_a isoline interval is 2 mS/m. Apparent conductivity is relatively low and invariable across most of the watershed. These characteristics reflect the resistive nature of the soils and parent rock that comprise the watershed. Within the watershed, EC_a averaged about 9.3 mS/m and ranged from 0.9 to 18.4 mS/m. One half the observations had values of EC_a between about 8.8 and 10.0 mS/m. In general, areas mapped as Weikert soil have an EC_a

less than 10 mS/m. Lower values of EC_a (6 to 8 mS/m) were largely recorded on convex shoulder and backslopes. Areas of lower EC_a (< 8 mS/m) have comparatively dry soil mantles that overlie resistive parent rock at very shallow depths. Areas of higher EC_a (> 10 mS/m) were recorded along the stream channel and recesses of the watershed. These areas include polygons of Earnest, Rushtown, and Blairton soils (Figure 2). These soils have higher moisture contents and deeper depths to bedrock. In a similar study conducted on a forested hillslope with variable depths to parent rock in southern New York, a high correlation was found between EC_a and soil moisture content (Sherlock and McDonnell, 2003).

While the two most conspicuous soil/landscape components (side slopes and drainageways) of the watershed were identified by the reconnaissance EMI survey, less extensive, more intricate soil/landscape patterns were omitted. Though initially assumed to be adequate, the number of EMI observations (N=2226) was too small and the traverse lines were too widely spaced to adequately identify and delineate the minor soil and topographic features of the watershed. The relatively broad area of wetter soils (Earnest and Blairton soils) along the stream channel and the drier and shallower to bedrock Weikert soil along upper back and shoulder slopes were distinguished by the reconnaissance EMI survey. However, as many soil and landscape components were not traversed with the EMI meter, many minor features are omitted or not clearly defined (Figure 4). The recesses of very deep, excessively drained Rushtown and moderately deep, well drained Berks soils, as well as convex shoulder slopes of very shallow (< 25 cm) soils were poorly defined. This is unfortunate as these features influence the flow of ground water within the watershed. Compared with surveys conducted on more level terrains that consist of broader soil and landscape units that grade gradually into one another, a greater number of more closely-spaced traverse lines is recommended for surveys conducted on topographically diverse terrains that contain smaller, more intricate soil patterns that are separated by relatively abrupt boundaries.

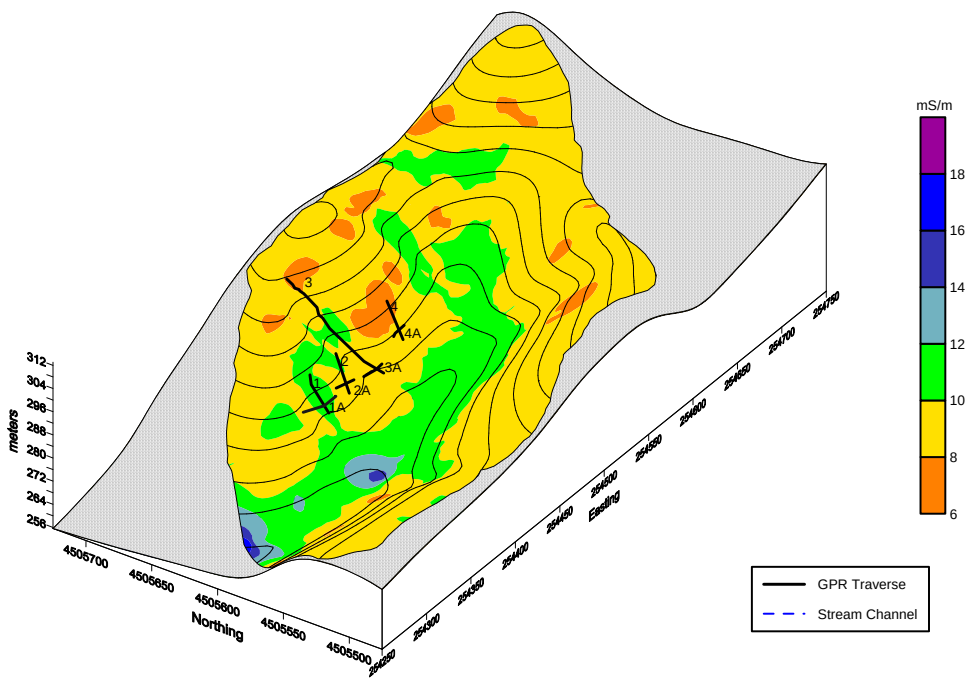

Figure 4. A map of apparent conductivity has been overlain on a topographic map of the watershed.

GPR Survey:

Based on the results of the high-intensity soil and reconnaissance EMI surveys, two conspicuous soil/landscape units, concave recesses of Rushtown and Berks soils and linear to slightly convex side slopes of Weikert soil were selected for more detailed investigations with GPR. A modest number of GPR traverses were conducted across representative areas of each of these features. The locations of these lines are shown in figures 3 and 4. In general, penetration depths and resolution of subsurface features were adequate for the determination of soil depths. However, because of the number and complexity of subsurface reflectors, the interpretation of the soil/bedrock interface was challenging and ambiguous in some areas.

The depth to bedrock influences the flow or water. Table 2 summarizes the interpreted depth to parent rock along traverse lines conducted on different landscape components.

Table 2. Depth to Bedrock
(In meters)

	Recess 1	*Recess 2*	*Backslope 1*	*Backslope 2*
	(lines 1 & 1A)	*(lines 3 & 3A)*	*(lines 2 & 2A)*	*(lines 4 & 4A)*
N	23	42	18	18
Average	1.07	1.32	0.40	0.52
Standard Deviation	0.65	0.73	0.11	0.27
Minimum	0.25	0.29	0.29	0.29
Maximum	2.16	2.74	0.73	1.29
1st Quartile	0.37	0.47	0.32	0.39
2nd Quartile	1.69	1.78	0.46	0.54

Within the recesses, the average depth to bedrock was 123 cm with a standard deviation of 71cm. Within recesses, based on soil-depth classes, soils are 28 % shallow, 14 % moderately deep, 14 % deep, and 45 % very deep. On side slopes, the average depth to bedrock was 46 cm with a standard deviation of 21 cm. On side slopes, based on soil-depth classes, soils are 75 % shallow, 22 % moderately deep, and 3 % deep. An analysis of variance was used to test for significant differences in the depth to bedrock between the two landscape components: recesses and side slopes. The null hypothesis was that the average depth to bedrock is the same on both landscape components. Based on 101 observations, the averaged depth to bedrock was 95 cm. The averaged depth to bedrock was found to be significantly different ($P = 0.0001$; F-value = 40.12) between the two landscape components. Although the sample population was small, results indicate significant differences in the depth to bedrock between the two landscape components.

<u>Radar records from a linear backslope of Weikert Soil:</u>
Lines 2, 2A, 4, and 4A (Figure 3 or 4) are confined to two linear side slopes of the watershed. These slopes are dominated by Weikert soil. Figure 5 is a 29-m portion of GPR traverse line 4. Line 4 is 30-m long and consists of 11 reference points. Relief along the line is about 7.0 m. The lower terminus of this line abutted the excavated pit of Weikert soil (see description 04PA061004). In Figure 5, a green line highlights the interpreted soil/parent rock interface. Along this traverse line, the depth to bedrock averages 51 cm with a range of 27 to 139 cm. A majority (>80%) of the observations have bedrock depths between 28 and 62 cm. No indication of bedrock depths can be understood from an analysis of slope form. Based on soil-depth criteria, this traverse line is 73% shallow, 18% moderately deep, and 9% deep soils.

In areas where the depth to bedrock is less than 35 cm, the soil/parent rock interface is partially obscured by multiples of the strong surface reflection. Though partially obscured, depths to bedrock were inferred to shallower depths based on trends and appearance of near surface reflections. On most radar records, the soil/ parent rock interface was clearly identifiable at depths greater than 40 cm. Below the soil/bedrock interface, the bedrock appears reflection-less. Reflections that appear in the lower part of the radar record (below depths of 1.6 to 2 m) represent noise. Within the watershed, bedding planes are inclined, fractured, and closely spaced. Because of the size of the propagating wavelengths (about 35 cm and 28 cm with the 200 and 400 MHz antennas, respectively), and the small contrast in electrical properties and the geometry (size, shape, orientation) of the shale beds, there is little scattering (reflected, refracted or diffracted) of the propagating electromagnetic wave. As a consequence, the bedrock appears reflection-less.

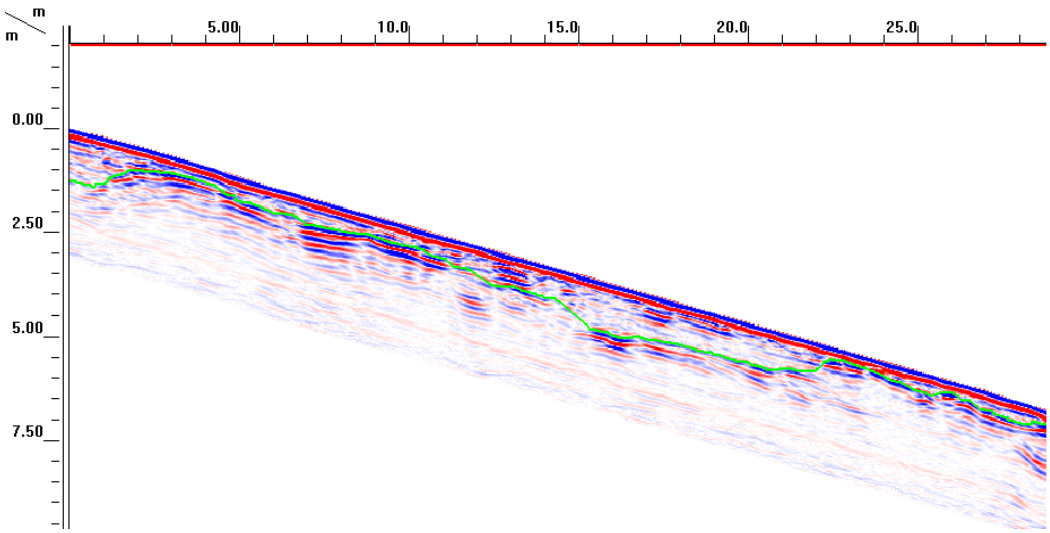

Figure 5. Interpreted depth to bedrock along Line 4.

<u>Radar records from a concave recess of Rushtown and Berks Soil:</u>
Lines 1, 1A, 3, and 3A (Figure 3 or 4) are confined to two recesses. Figure 6 is a 28-m portion of GPR traverse line 1. This traverse was conducted down the long axis of a recess. This line is 30-m long and consists of 11 flagged reference points that are spaced at an interval of about 3 m. Relief along the line is about 11.7 m. In Figure 6, a green line highlights the interpreted soil/parent rock interface. Along this traverse line, the depth to bedrock averages 145 cm with a range of 32 to 216 cm. A majority (>80%) of the observations have bedrock depths between 44 and 192 cm. In general, the depth to bedrock is shallowest near the head of the recess and deepens rapidly in a down slope direction. Throughout most of the recess the depth to bedrock remains fairly constant and is very deep. Undulations in the surface appear to coincide with undulations in the bedrock surface. Based on soil-depth criteria, this traverse line is 18% shallow, 18% deep, and 64% very deep soils.

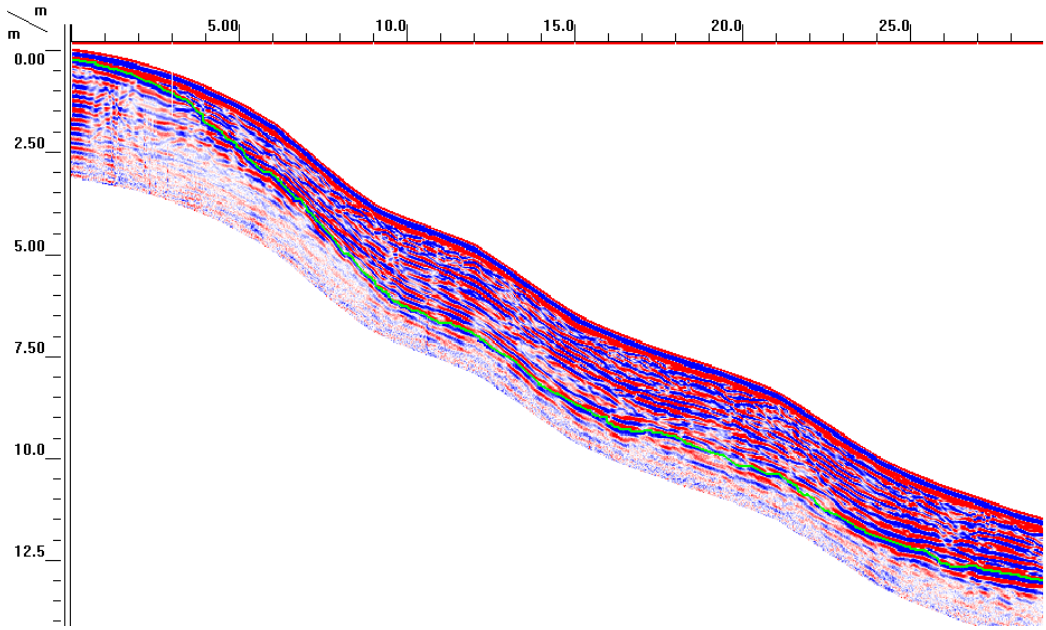

Figure 6. Interpreted depth to bedrock along the long axis of a recess (Line 1).

In Figure 6, in the upper 3-m of GPR traverse line, the depth to bedrock is shallow. This portion of the traverse line crosses the convex shoulder slope at the head of the recess. Here the reverberations of the surface pulse obscure the soil/parent rock interface. Near the 4-m mark, the soil/parent rock interface plunges as the backslope of the recess is entered. Near the 7-m mark, the sideslopes of the recess become more pronounced and the soil deepens over parent rock (see Figure 6). Over a lateral distance of 3-m the soil deepen by about 2-m and rather abruptly transitions from shallow Weikert soil to very deep Rushtown soil. The recess is filled with slightly wavy, high-amplitude linear reflectors, which represent beds of colluvium. These layers are continuous over short distances and undoubtedly influence the flow of water.

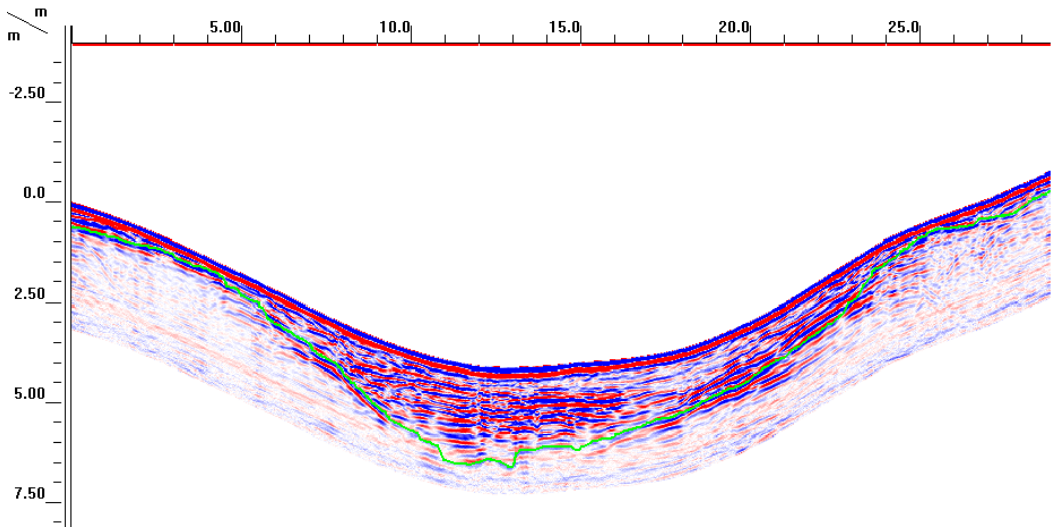

Figure 7. Interpreted depth to bedrock across a recess (Line 3A).

Figure 7 is a 29-m portion of GPR traverse line 3A. This traverse line is 33-m long and consists of 12 reference points. This traverse was conducted orthogonal to the axis of the recess. Relief along the line is about 12.2 m. The traverse line is adjacent to the excavated pits of Rushtown and Berks soil. In Figure 7, a green line highlights the interpreted soil/parent rock interface. The convex shoulder slopes, which form the edges to the recess, are dominated by Weikert soil. Moderately deep Berks soil is restricted to the upper portions of the steep side slopes to the recess. The concave recess bottom is dominated by Rushtown soil. A series of high-amplitude linear reflectors characterize areas of Rushtown soil. These reflectors represent sequential layers of colluvium. These layers influence the movement of soil moisture. Along this traverse line, the depth to bedrock averages 76 cm with a range of 32 to 185 cm. A majority (>80%) of the observations have bedrock depths between 33 and 160 cm. Based on soil-depth criteria, this traverse line is 33% shallow, 25% moderately deep, 8% deep and 33% very deep soils.

Line 3 (Figure 3 or 4) follows the centerline of the long axis of a large recess. The traverse line is 87-m long. Figures 8 and 9 show the upper 29-m and lower 27-m of this traverse line, respectively. Though the size and length of this recess are larger, the same sequence of soil features is evident in this recess as in the smaller recess represented by GPR traverse line 1 (Figure 6).

The convex shoulder slopes at the head of this large recess is shown in Figure 8. The depth to bedrock is shallow across the convex shoulder slopes at the head of this recess. Here the strong surface pulse obscures the very shallow and shallow soil/bedrock interface. Between the 18 and 24-meter marks, the depth to bedrock becomes moderately deep and the soil is Berks. Below the 24-m mark the depth to bedrock deepens fairly precipitously in a down slope direction. Along this backslope component to the recess, subsurface interfaces are of intermediate amplitude suggesting layers with closely similar electromagnetic and soil properties. These layers of colluvium appear discontinuous and ill-defined.

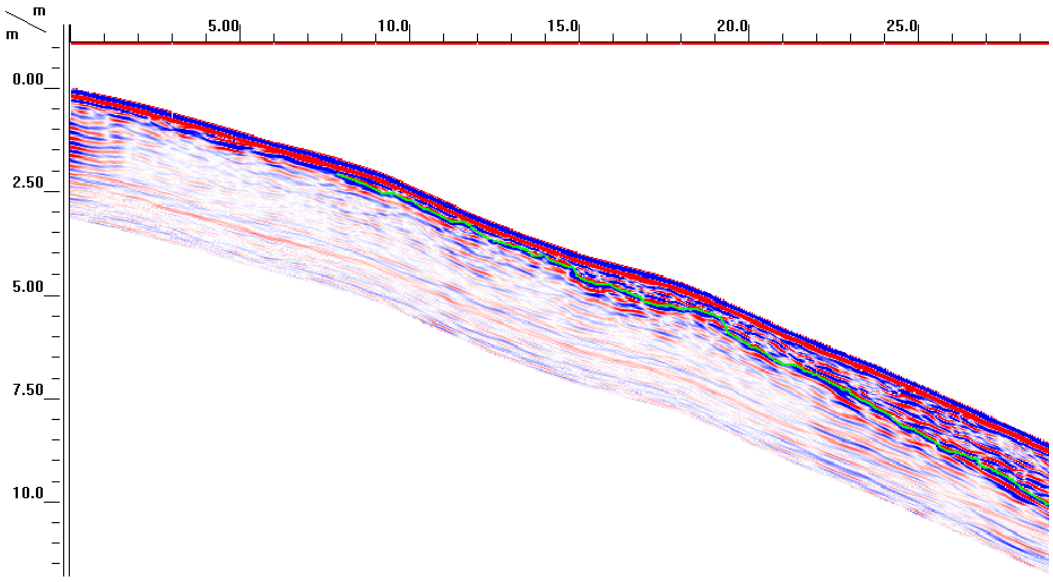

Figure 8. In the upper part of the recess, depth to bedrock deepens and layers of colluvium thicken over short distances.

Figure 9 is the radar record from the lower portion (60- to 87-m) of the traverse conducted along the long axis of the large recess. Along this toeslope, the depth to bedrock averages 149 cm and ranges from 124 to 167 cm. Compared with the area along the head of this recess (Figure 8), the depth to bedrock is remarkably deep and uniform along the toeslope of the recess. The pit of Rushtown soil (04PA061002) is located near the 84-m mark. Here the interpreted depth to bedrock is about 210 cm. The bedrock appears to consist of a series of broad, slightly inclined steps, which are bounded by narrow, more steeply inclined risers. Numerous, inclined, segment, weak to high amplitude, linear interfaces are evident above the soil/parent rock interface. These subsurface interfaces represent sequential layers of colluvium. These layers influence the movement of soil moisture.

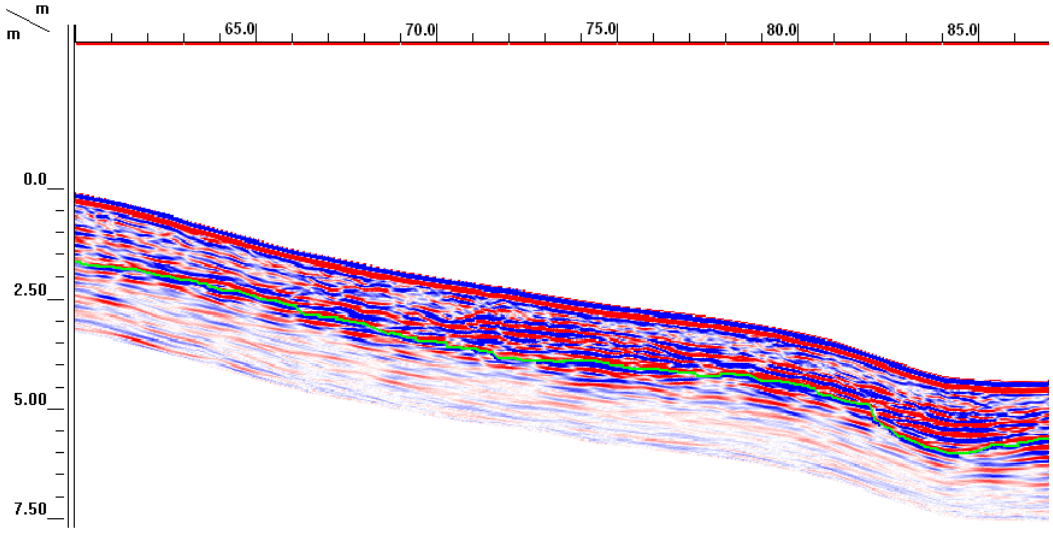

Figure 9. Layers of colluvium are evident along the toeslope to the recess along Line 3.

3D images:

The form and geometry of subsurface features can be studied in two-dimensional, intersecting radar records (van Heteren et al., 1998). Recently, with the advent of digital GPR outputs and advanced data processing software, it has become possible to analyze the structure or configuration of subsurface features in three-dimensions (3D). Under favorable

conditions, GPR and 3D imaging can provide additional information and perspectives into the subsurface. The acquisition of data for 3D images requires greater resources than the collection of 2D radar records. To construct 3D images, a relatively small area is intensively surveyed with closely spaced (often <1 m), parallel GPR traverses. Data from these lines are processed into a 3D image. Once processed, arbitrary cross-sections, insets, and time slices can be extracted from the 3D data set. The flexibility of 3D visualizations can facilitate the interpretation of spatial relationships and the analysis of soil, structural, and/or stratigraphic features. This imaging technique enables views of the subsurface from nearly any perspective (Junck and Jol, 2000). Detailed radar investigations of small selected areas and the construction of 3D imagery may improve our knowledge of the variability of soils and soil properties within the Shale Hills Watershed.

Figures 10, 11, and 12 are 3D cutout cube images of radar data collected from grids located along different portions of the large recess and traverse line 3. The locations of the three grids are shown in Figure 3. Each grid was located in a relatively open area along the center line of the recess. Slopes were relatively gentle and uniform within each grid. Because of limitations in the processing software, the radar data could not be surface normalized (data corrected for changes in surface elevation) without the surface layers being hidden from view in the 3D cubes. Therefore, each cube has been rotated and tilted to approximate the slope of the ground surface. In each plot, the X-axis is parallel and the Y-axis is orthogonal with the slope.

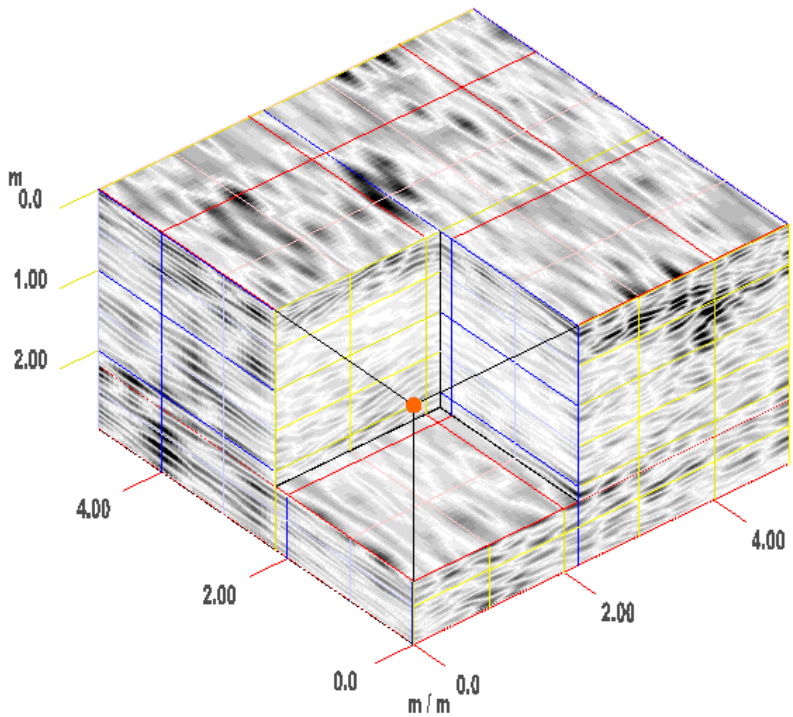

Figure 10. Low amplitude reflections characterize the 3D cutout cube from the convex shoulder slope at the head of a recess.

The 3D cutout cube image shown in Figure 10 is from the shoulder slope at the head of the recess. This area is dominated by Weikert soil. Reflections are of low to moderate amplitudes suggesting earthen materials with similar electromagnetic properties. The soil/bedrock interface is barely perceptible in the upper part (0 to 50 cm depth) of the cube. Very low amplitude reflections and bands of noise characterize the underlying shale bedrock.

The 3D cutout cube image shown in Figure 11 is from the backslope section of the recess. This area is dominated by Rushtown and Berks soils. Compared with the 3D cutout cube from the convex shoulder slope (Figure 10), reflections are higher in amplitude and more noticeable suggesting earthen materials with more dissimilar electromagnetic properties. The soil/bedrock interface varies in depth from about 210 to 230 cm in this cube and is barely distinguishable from the overlying strata. The overlying strata are characterized by comparatively short (about 1-m), imbricating layers that are

inclined in a down slope direction. These strata appear to be more extensive along the Y-axis (orthogonal to slope). The comparatively high amplitudes of these interfaces suggest contrasting materials. These contrasts probably reflects variations in moisture content; the result of differences in grain-size distributions, density, and/or rock fragments.

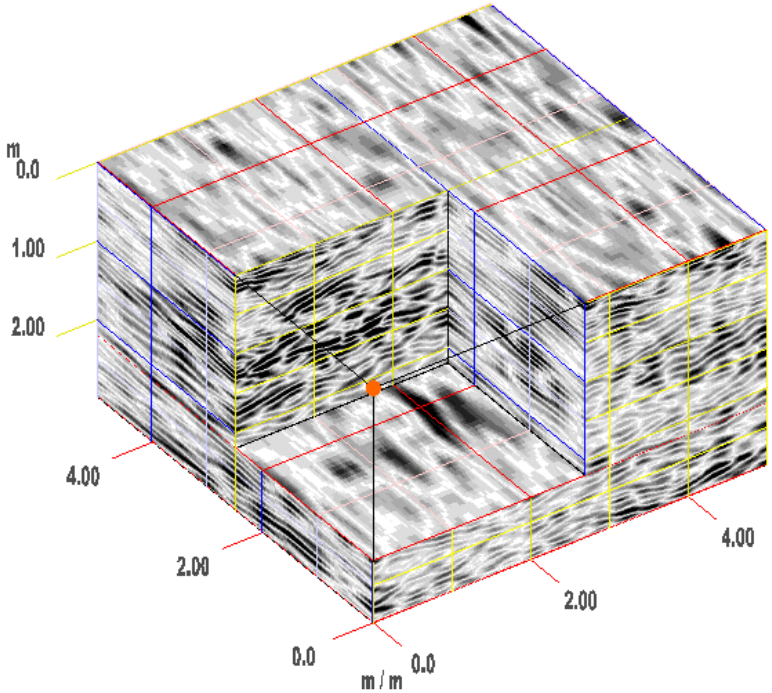

Figure 11. Moderate amplitude reflections characterize the colluvium in this 3D cutout cube from the mid-slope section of a large recess.

The 3D cutout cube image shown in Figure 12 is from the toeslope section of the recess. This area is dominated by Rushtown and Berks soils. Compared with the other 3D cutout cubes (Figures 10 and 11), subsurface reflections are more numerous and noticeably higher in amplitude. The higher amplitudes are believed to be caused by higher contrast in soil moisture contents between the layers of colluvium. The soil/bedrock interface is at a depth of about 200 cm. Interfaces are apparent within the bedrock. In general, interfaces within the shale bedrock were of lower amplitude or were not apparent on higher-lying slopes of the watershed. As in the cube from the linear backslope section of the recess, the overlying colluvium is characterized by comparatively short (about 1-m), overlapping layers, which are inclined in a down slope direction. These strata are more extensive along the Y-axis (orthogonal to slope). The comparatively high amplitudes of these interfaces suggest materials that contrast in moisture content, grain-size distributions, density, and/or rock fragments.

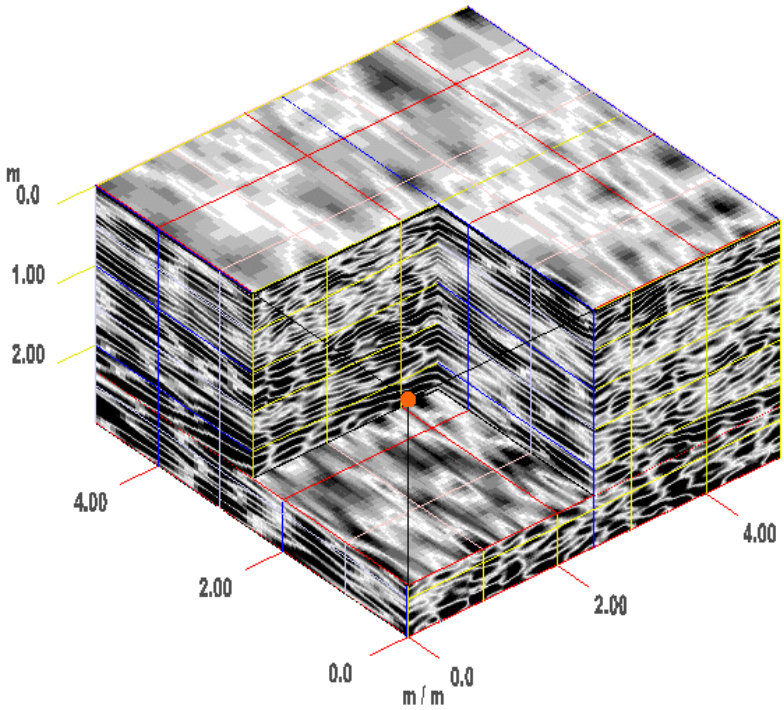

Figure 12. High amplitude reflections characterize moister colluvial deposits in this 3D cutout cube from the toeslope section of a large recess.

References:

Bohling, G. C., Anderson, M. P. and Bentley, C. R. 1989. Use of ground penetrating radar to define recharge areas in the Central Sand Plain. Technical Completion Report G1458-03. Geology and Geophysics Department, University of Wisconsin-Madison, Madison, Wisconsin.

Collins, M. E., J. A. Doolittle, and R. V. Rourke. 1989. Mapping depth to bedrock on a glaciated landscape with ground-penetrating radar. Soil Science Society of America J. 53:1806-1812.

Daniels, D. J. 2004. Ground Penetrating Radar; 2nd Edition. The Institute of Electrical Engineers, London, United Kingdom.

Davis, J. L. and A. P. Annan. 1989. Ground-penetrating radar for high resolution mapping of soil and rock stratigraphy. Geophysical Prospecting 37:531-551.

Doolittle, J. A. 1987. Using ground-penetrating radar to increase the quality and efficiency of soil surveys. 11-32 pp. IN Soil Survey Techniques, Soil Sci. Soc. Am. Special Pub. No 20.

Doolittle, J. A., B. J. Jenkinson, D. P. Franzmeier and W. Lynn. 2000. Improved Radar Interpretations of Water-table depths and Ground-water flow patterns Using Predictive Equations. In: D. Noon (Editor) Proceedings Eight International Conference on Ground-Penetrating Radar. May 23 to 26, 2000, Goldcoast, Queensland, Australia. The University of Queensland, pp. 488-495.

Doolittle, J., R. Murphy, G. Parks, and J. Warner. 1996. Electromagnetic induction investigations of a soil delineation in Reno County, Kansas. Soil Survey Horizons 37:11-20.

Doolittle, J. A., K. A. Sudduth, N. R. Kitchen, and S. J. Indorante. 1994. Estimating depth to claypans using electromagnetic inductive methods. J. Soil and Water Conservation 49(6):552-555.

Geonics Limited. 1998. EM38 ground conductivity meter operating manual. Geonics Ltd., Mississauga, Ontario.

Greenhouse, J. P., and D. D. Slaine. 1983. The use of reconnaissance electromagnetic methods to map contaminant migration. Ground Water Monitoring Review 3(2): 47-59.

Inman, D. J., R. S. Freeland, J. T. Ammons, and R. E. Yoder. 2002. Soil Investigations using electromagnetic induction and ground-penetrating radar in southwest Tennessee. Soil Science Society of America J. 66: 206-211.

Iivari, T. A. and J. A. Doolittle. 1994. Computer simulations of depths to water table using ground-penetrating radar in topographically diverse terrains. In: K. Kovar and J. Soveri (Editors). Ground water Quality Management (Proceedings of GQM 93, International Association of Hydrological Sciences, Tallinn, Estonia. September 1993, pp. 11-20.

Jaynes, D. B. 1995. Electromagnetic induction as a mapping aid for precision farming. pp. 153-156. IN: Clean Water, Clean Environment, 21st Century: Team Agriculture. Working to Protect Water Resources. Kansas City, Missouri. 5 to 8 March 1995.

Jaynes, D. B., T. S. Colvin, J. Ambuel. 1993. Soil type and crop yield determination from ground conductivity surveys. 1993 International Meeting of American Society of Agricultural Engineers. Paper No. 933552. ASAE, St. Joseph, MI.

Junck, M. B. and H. M. Jol. 2000. Three-dimensional investigation of geomorphic environments using ground penetrating radar. 314-318 pp. IN: (Noon, D. Ed.) Proceedings Eight International Conference on Ground-Penetrating Radar. May 23 to 26, 2000, Gold Coast, Queensland, Australia. The University of Queensland.

Kravchenko, A. N., G. A. Bollero, R. A. Omonode, and D. G. Bullock. 2002. Quantitative mapping of soil drainage classes using topographical data and soil electrical conductivity. Soil Science Society of America J. 66:235-243.

Merkel, E. 1978. Soil Survey of Huntingdon County, Pennsylvania. USDA-Soil Conservation Service in cooperation with Pennsylvania State University College of Agriculture and the Pennsylvania Department of Environmental Resources and State Conservation Commission. Government Printing Office, Washington DC.

Olson, C. G. and J. A. Doolittle. 1985. Geophysical techniques for reconnaissance investigations of soils and surficial deposits in mountainous terrain. Soil Science Society of America J. 49: 1490-1498.

Sherlock, M. D. and J. J. McDonnell. 2003. A new tool for hillslope hydrologists: spatially distributed groundwater level and soilwater content measured using electromagnetic induction. Hydrological Processes 17: 1965-1977.

Stroh, J. C., S. Archer, J. A. Doolittle, and L. Wilding. 2001. Detection of edaphic discontinuities with ground-penetrating radar and electromagnetic induction. Landscape Ecology 16: 377-390.

Sudduth, K. A., N. R. Kitchen, D. H. Hughes, and S. T. Drummond. 1995. Electromagnetic induction sensing as an indicator of productivity on claypan soils. 671-681 pp. IN: Robert, P. C., R. H. Rust, and W. E. Larson (editors). Proceedings of Second International Conference on Precision Management for Agricultural Systems. Minneapolis, Minnesota. March 27-30, 1994. American Society of Agronomy, Madison, WI.

van Heteren, S., D. M. Fitzgerald, P. A. McKinlay, and I. V. Buynevich. 1998. Radar facies of paraglacial barrier systems: coastal New England, USA. Sedimentology, 43: 181-200.

Pedon ID: 04PA061002 RUSHTOWN
This pit is located in swale on the backslope of the hill. It is formed from colluvium.
Legal Description:
UTM Zone: 18
UTM Easting: 254461 meters
UTM Northing: 4505620 meters

Geomorphic Setting: on foot slope of None Assigned
Upslope Shape: concave Cross Slope Shape: concave

Oe--0 to 5 centimeters (0.0 to 2.0 inches); many fine roots throughout; abrupt smooth boundary.

A--5 to 11 centimeters (2.0 to 4.3 inches); black (10YR 2/1) broken face silt loam; strong fine granular structure; friable, nonsticky, nonplastic; many fine roots throughout; common fine dendritic tubular pores; 5 percent flat 2- to 150-millimeter shale fragments; very strongly acid, pH 4.5, Hellige-Truog; abrupt smooth boundary.

Bw1--11 to 17 centimeters (4.3 to 6.7 inches); brown (7.5YR 4/4) broken face silt loam; weak medium subangular blocky structure; friable, nonsticky, nonplastic; common fine roots throughout; common fine dendritic tubular pores; 5 percent flat 2- to 150-millimeter shale fragments; very strongly acid, pH 4.5, Hellige-Truog; clear smooth boundary.

Bw2--17 to 26 centimeters (6.7 to 10.2 inches); reddish brown (5YR 4/4) broken face sandy loam; weak medium subangular blocky structure; friable, nonsticky, nonplastic; common fine and medium roots throughout and common coarse roots throughout; common fine dendritic tubular pores; 5 percent flat 2- to 150-millimeter shale fragments; very strongly acid, pH 4.5, Hellige-Truog; clear smooth boundary.

Bw3--26 to 38 centimeters (10.2 to 15.0 inches); yellowish red (5YR 4/6) broken face silty clay loam; weak medium subangular blocky structure; friable, slightly sticky, nonplastic; common fine and medium roots throughout and common coarse roots throughout; few very fine dendritic tubular pores; 5 percent flat 2- to 150-millimeter shale fragments; very strongly acid, pH 4.5, Hellige-Truog; clear smooth boundary.

BC--38 to 60 centimeters (15.0 to 23.6 inches); yellowish red (5YR 4/6) broken face very channery silty clay loam; massive; friable, slightly sticky, slightly plastic; few medium roots throughout; few very fine dendritic tubular pores; 50 percent flat 2- to 150-millimeter shale fragments; very strongly acid, pH 4.5, Hellige-Truog; clear smooth boundary.

C--60 to 182 centimeters (23.6 to 71.6 inches); strong brown (7.5YR 4/6) broken face extremely channery silty clay loam; massive; friable, slightly sticky, slightly plastic; 80 percent flat 2- to 150-millimeter shale fragments; very strongly acid, pH 4.5, Hellige-Truog.

Pedon ID: 04PA061003 BERKS
Legal Description:
UTM Easting: 254466 meters
UTM Northing: 4505621 meters

Geomorphic Setting: on backslope of backslope of None Assigned
Upslope Shape: Cross Slope Shape:

Oe--0 to 5 centimeters (0.0 to 2.0 inches); many fine roots throughout; many fine tubular pores; abrupt smooth boundary.

A--5 to 8 centimeters (2.0 to 3.1 inches); reddish brown (5YR 4/3) broken face silt loam; moderate fine granular structure; friable, slightly sticky, nonplastic; many fine roots throughout; many fine tubular pores; very strongly acid, pH 4.5, Hellige-Truog; clear smooth boundary.

Bw1--8 to 14 centimeters (3.1 to 5.5 inches); brown (7.5YR 4/4) broken face silt loam; weak very fine subangular blocky structure; friable, slightly sticky, nonplastic; many medium roots throughout; many medium tubular pores; 2 percent flat 2- to 150-millimeter shale fragments; very strongly acid, pH 4.5, Hellige-Truog; clear smooth boundary.

Bw2--14 to 53 centimeters (5.5 to 20.9 inches); strong brown (7.5YR 4/6) broken face silt loam; weak fine subangular blocky structure; friable, slightly sticky, nonplastic; many medium roots throughout; many medium tubular pores; 2 percent flat 2- to 150-millimeter shale fragments; very strongly acid, pH 4.5, Hellige-Truog; clear smooth boundary.

Bw3--53 to 69 centimeters (20.9 to 27.2 inches); strong brown (7.5YR 4/6) broken face very channery silty clay loam; weak fine subangular blocky structure; friable, slightly sticky, nonplastic; many medium roots throughout; many medium tubular pores; 50 percent flat 2- to 150-millimeter shale fragments; very strongly acid, pH 4.5, Hellige-Truog; clear smooth boundary.

C--69 to 145 centimeters (27.2 to 57.1 inches); yellowish red (5YR 4/6) broken face extremely channery silty clay loam; massive; friable, slightly sticky, nonplastic; few fine roots throughout; few fine tubular pores; 90 percent flat 2- to 150-millimeter shale fragments; very strongly acid, pH 4.5, Hellige-Truog; abrupt smooth boundary.

R--145 centimeters (57.1 inches).

Pedon ID: 04PA061004 WEIKERT
Legal Description:
UTM Easting: 254491 meters
UTM Northing: 4505623 meters
Geomorphic Setting: on backslope of backslope of None Assigned
Upslope Shape: convex Cross Slope Shape: linear

Oe--0 to 5 centimeters (0.0 to 2.0 inches); many fine roots throughout; many fine tubular pores; extremely acid, pH 4.0, Hellige-Truog; abrupt smooth boundary.

A--5 to 12 centimeters (2.0 to 4.7 inches); dark brown (7.5YR 3/2) broken face silt loam; moderate fine granular structure; friable, nonsticky, nonplastic; many fine roots throughout; many fine tubular pores; very strongly acid, pH 4.5, Hellige-Truog; clear smooth boundary.

Bw--12 to 24 centimeters (4.7 to 9.4 inches); yellowish red (5YR 4/6) broken face very channery silt loam; moderate fine granular structure; friable, slightly sticky, nonplastic; many fine roots in cracks; many fine tubular pores; 60 percent flat 2- to 150-millimeter shale fragments; very strongly acid, pH 4.5, Hellige-Truog; clear smooth boundary.

C--24 to 37 centimeters (9.4 to 14.6 inches); yellowish red (5YR 4/6) broken face extremely channery silt loam; weak fine subangular blocky structure; friable, slightly sticky, nonplastic; few fine roots in cracks; few fine tubular pores; 90 percent flat 2- to 150-millimeter shale fragments; very strongly acid, pH 4.5, Hellige-Truog; clear smooth boundary.

R--37 centimeters (14.6 inches).